CHIN. PHYS. LETT. Vol. 32, No. 9 (2015) 096102

Electronic and Optical Properties of TiS_2 Determined from Generalized Gradient Approximation Study

Hamza El-Kouch[1], Larbi El Farh[1**], Jamal Sayah[1], Allal Challioui[2]

[1]*Laboratoire de mécanique & énergétique, Département de Physique, Faculté des Sciences, Université Mohammed Premier, Oujda, Maroc*

[2]*Laboratoire de chimie organique macromoléculaire et produits naturels, Equipe: Photochimie et Chimie Macromoléculaire, Faculté des Sciences, Université Mohammed Premier, Oujda, Maroc*

(Received 2 June 2015)

The electronic and optical properties of TiS_2 are studied by using an ab-initio calculation within the frame of density functional theory. A linearized and augmented plane wave basis set with the generalized gradient approximation as proposed by Perdew et al. is used for the energy exchange-correlation determination. The results show a metallic character of TiS_2, and the plots of total and partial densities of states of TiS_2 show the metallic character of the bonds and a strong hybridization between the states d of Ti and p of S below the Fermi energy. The optical properties of the material such as real and imaginary parts of dielectric constant ($\varepsilon(\omega) = \varepsilon_1(\omega) + i\varepsilon_2(\omega)$), refractive index $n(\omega)$, optical reflectivity $R(\omega)$, for $E//x$ and $E//z$ are performed for the energy range of 0–14 eV.

PACS: 61.66.−f, 71.15.Mb, 71.20.−b DOI: 10.1088/0256-307X/32/9/096102

The titanium disulfide (TiS_2) is one of the layered transition-metal dichalcogenide (LTMD) materials consisting of covalently bonded Ti and S atoms arranged in two-dimensional hexagonal planes.[1−7] The layers are stacked together by weak van der Waals forces.[8] TiS_2 has been widely studied in recent years due to its use in numerous applications such as the cathode material in rechargeable batteries,[3,6,8−11] hydrogen storage material,[3,6,8,11] and as a high-performance thermoelectric material.[11,12] In the literature, there are many conflicting results on the electronic structure of TiS_2 since it is still debated whether the material is metallic, semi-metallic or semiconductor.[2,6,8,11,13−18] Several experimental works have reported that TiS_2 has semiconductor behavior with a band gap ranging from 0.05 to 2.5 eV.[4,9,11,12] At the same time, other experiments classify TiS_2 among metals[6,13] or semimetals[1,8,16−18] with an indirect band gap overlap ranging from 0.2 to 1.5 eV (between the points Γ and L in the first Brillouin zone). The aim of the present work is to report the results obtained in theoretical studies of the electronic, structural and optical properties of TiS_2 by using density functional theory (DFT) and full potential linearized and augmented plane wave (FLAPW) basis set.

Electronic and optical properties of TiS_2 were studied by using an FLAPW method, implemented in the WIEN2K code.[2,11] The calculations are based on DFT in the generalized gradient approximation (GGA) of the exchange and correlation potential in the simple formulation of Perdew *et al.*[19] The Muffin–Tin radii are set to 2.34 Å and 2.08 Å for Ti atoms and S atoms, respectively, and the cutoff energy is −6.0 Ry between the valence and the core states. The plane waves cutoff parameter is $R_{\rm mt} \cdot K_{\rm max} = 9$, and the highest orbital momentum $l_{\rm max} = 10$ is used in all calculations. The number of the k points inside the irreducible Brillouin zone is 900. The titanium disulfide TiS_2 is one of the transition metal dichalcogenides that crystallizes in the CdI_2 system ($P-3m1$, space group No.164)[19] corresponding to the atomic positions listed in Table 1. One Ti atom is located at 1a (0, 0, 0) and two S atoms at 2d (1/3, 2/3, 1/4) and (2/3, 1/3, 3/4) in the unit cell (Fig. 1). Table 1 lists the optimized lattice parameters of the compound under study and the experimental bulk ones.[20]

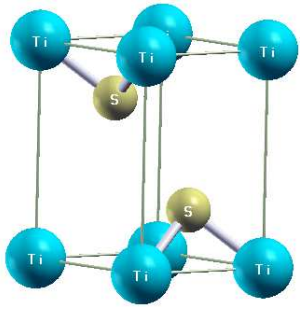

Fig. 1. Unit cell of TiS_2.

Table 1. Structure parameters and atomic positions for TiS_2.

	a (Å)	b (Å)	c (Å)	α (deg)	β (deg)	γ (deg)
Present	3.31	3.31	5.55	90	90	120
Expt.[20]	3.407	3.407	5.695			

Figure 2 presents the total energy variation as a function of the volume for TiS_2 obtained from the GGA calculation. The curve total energy-volume was fitted to the Murnaghan–Birch equation of state[21] to determine the equilibrium structural parameters. The calculated equilibrium volume V_0, bulk modulus B_0, pressure derivative B_0' and ground state energy E_0 are

**Corresponding author. Email: elfarhlarbi@yahoo.fr

© 2015 Chinese Physical Society and IOP Publishing Ltd

collected in Table 2. The bulk modulus B_0 is a measure of the crystal rigidity, thus a large value of B_0 indicates a high crystal rigidity.

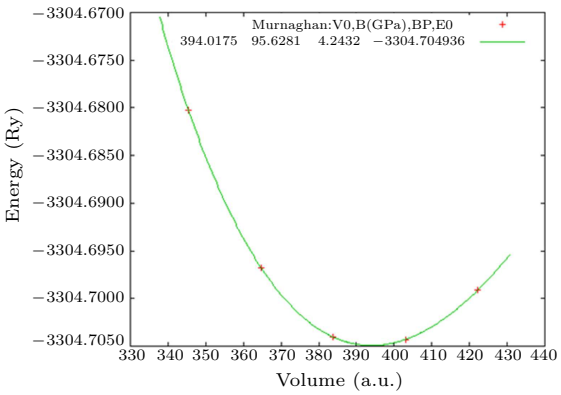

Fig. 2. Total energy–volume curve for TiS_2 within GGA.

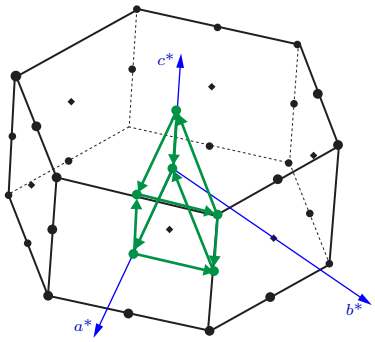

Fig. 3. Brillouin zone and high-symmetry points for TiS_2.

Table 2. Structural parameters derived from the Murnaghan–Birch equation of state.

	V_0 (Å^3)	B_0 (GPa)	B_0'	E_0 (Ry)
Present	59.10	95.6281	4.2432	−3304.704936
Expt.[8]	57.24	45.90	9.50	
Theor.[8]	51.72	58.91	4.11	

The density of state (DOS) components were calculated for the Ti atom, the S atom and the total density of states of TiS_2 within Muffin-Tin spheres (MT). Figure 4(a) shows the profile of the total density of states of TiS_2, partial and total densities of states of s, p and d levels of both sulfur and titanium atoms. The Fermi energy E_F was reduced to 0 eV in these figures and is indicated with the vertical dashed line. The DOS could be mainly divided into four parts: the first part extending from −12 to −11.5 eV consists mainly of the S s states, the second from −5.5 to 0 eV and the third from 0 to 4.0 eV are mainly the contribution of the Ti d states and the S p states, and the last part from 6 to 15.0 eV mainly contains mixtures of the S p states and the Ti d states. The DOS at the Fermi level is controlled by the overlap between the states p of S and d of Ti. The existence of a very strong hybridization between the Ti d states and the S p states is also observed below the Fermi energy in the region from 0 to −5.0 eV. The band structure was calculated through the k-path of high symmetry points in the first Brillouin zone (Fig. 3). Figure 4(b) shows the band structure of TiS_2. From this figure, some overlap between the conduction band and the valence band, as the minimum of the conduction band, is below the Fermi level E_F at the L point and the maximum of the valence band is above the Fermi level E_F in the Γ point, which is consistent with a metal character of TiS_2. More accurate results should take into account the van der Waals correction, while in this work we give a comparison of our results with the literature.

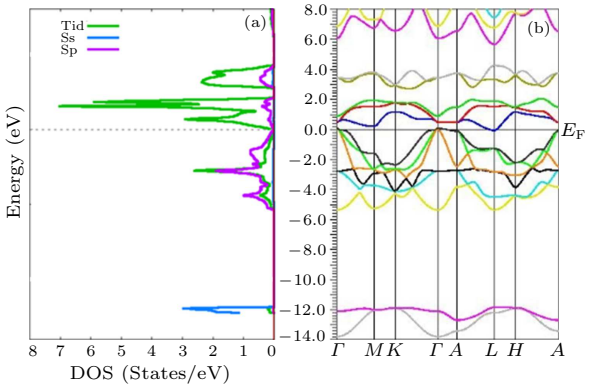

Fig. 4. (a) Partial electronic density of states and (b) electronic band structures of TiS_2.

Optical properties of materials can be described by the complex dielectric function $\varepsilon(\omega)$, which represents the linear response of a system to an external electromagnetic field with a small wave vector.[22] It can be expressed as

$$\varepsilon(\omega) = \varepsilon_1(\omega) + i\varepsilon_2(\omega), \tag{1}$$

where $\varepsilon_1(\omega)$ and $\varepsilon_2(\omega)$ are the real and the imaginary parts of the dielectric function, respectively. Figure 5(a) shows the calculated real part of the complex dielectric function ε_1 of TiS_2 for $E//x$ and $E//z$, respectively. It is clear from the figure that the static dielectric constant $\varepsilon_1(0)$ and the low energy limit of ε_1 are strongly dependent on the bandgap of the compound. The inverse relation of $\varepsilon_1(0)$ with the band gap can be explained by the Penn model,[23]

$$\varepsilon_1(0) \approx 1 + (\hbar\omega_p/E_g)^2, \tag{2}$$

which can be used to calculate E_g using $\varepsilon_1(0)$ and the plasma energy $\hbar\omega_p$. It is evident from Fig. 5(a) that the first hump for TiS_2 appears at 0.57 eV and 0.9 eV for $E//x$ and $E//z$, respectively, ε_1 becomes zero at a certain energy and then decreases to the minimum values of 4.76 eV and 5.62 eV for $E//x$ and $E//z$, respectively. The negative values of ε_1 show that in this energy region the incident electromagnetic waves are totally reflected from the medium, hence the material exhibits a metallic nature. The negative values of ε_1 correspond to the local maxima of the reflectivity (can be confirmed by Fig. 6(b)). Additional increase in the energy to a high value brings steadiness to $\varepsilon_1(\omega)$. The stable behavior after 10 eV suggests that the studied material does not interact with these high energy photons as it is transparent to them and thus is suitable

for manufacturing lenses. Figure 5(b) shows the calculated imaginary part of the dielectric function of TiS_2 for $E//x$ and $E//z$ for the energy range of 0–14 eV. The main contributions to the optical spectra originate from the top valence bands to the lower conduction bands. The edge of optical absorption in TiS_2 occurs at about 0, 31 eV and 0.67 eV for $E//x$ and $E//z$, respectively. This position is the valence band and the conduction band splitting at Γ and L points ($\Gamma_V - L_C$), which gives the threshold for the direct optical transition between the highest valence band and the lowest conduction band. This is known as the fundamental absorption edge. It is also clear from the figure that TiS_2 has three main structures labeled A, B, and C. The location of these structures in the TiS_2 compound is given in Table 3. Structure A is dominated by transitions from a band just below E_F to a band just above it in the M direction. Structures B and C are dominated by transitions from the top (and bottom) of the chalcogen p states to Ti d states. The width of the absorption region depends on the bandgap of the material. The variation of the peak magnitudes of the absorption region with energy confirms the suitability of the studied material for device applications in different parts of the spectrum.

Table 3. Peak positions of ε_2 for TiS_2 compound (all in eV).

	A	B	C
TiS_2	1.5	4.2	9.2

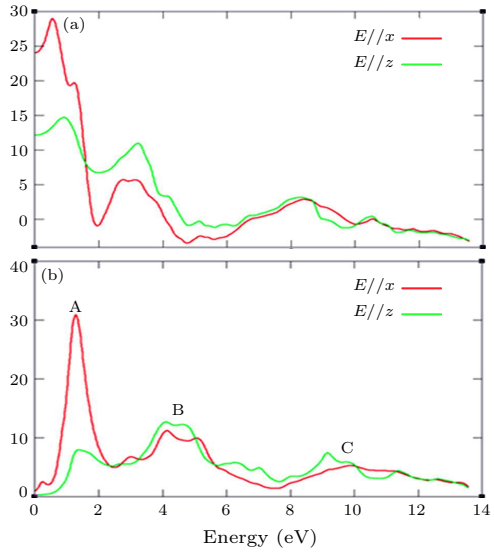

Fig. 5. (a) The real part ε_1 and (b) the imaginary part ε_2 of the dielectric function of TiS_2 within GGA.

Figure 6(a) shows a broad spectrum of refractive index $n(\omega)$ for TiS_2 for $E//x$ and $E//z$, for the energy range of 0–14 eV. The index $n(\omega)$ closely follows the real part of the complex dielectric function $\varepsilon_1(\omega)$. The calculated refractive index at zero frequency limits for TiS_2 is listed in Table 4. The refractive index reaches the maxima about 0.61 eV and 0.97 eV for $E//x$ and $E//z$, respectively. The refractive index is greater than one due to the fact that as photons enter a material they are slowed down by the interaction with electrons. The more photons are slowed down while traveling through a material, the greater the material's refractive index. Generally, any mechanism that increases the electron density in a material also increases the refractive index. The refractive index of the compound starts decreasing beyond the maximum value and goes below one for the range given in Table 4. A refractive index of less than unity ($V_g = c/n$) shows that the group velocity of the incident radiation is greater than c. Figure 5(b) shows the relationship between reflectivity (frequency dependent) $R(\omega)$ and energy for TiS_2 for $E//x$ and $E//z$, respectively, with the GGA. The magnitude of the reflectivity for TiS_2 at zero frequency is given in Table 4. The maximum reflectivity about 13.58 eV for $E//x$ and $E//z$, i.e., the minimum value $\varepsilon_1(\omega)$ will occur. From Fig. 6(b), the reflectivity is greater for high energy incident beam, thus the corresponding waves are reflected and do not produce interband transition.

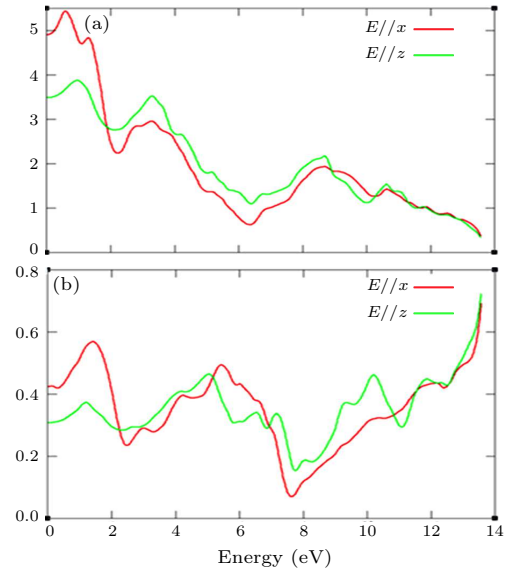

Fig. 6. (a) Frequency-dependent refractive indices. (b) Reflectivity (frequency dependent) of TiS_2 within GGA.

Table 4. Calculated zero frequency limits of the real part of dielectric constant $\varepsilon_1(0)$, the imaginary part of dielectric constant $\varepsilon_2(0)$, refractive index $n(0)$, reflectivity $R(0)$, energy range for $n(\omega) < 1$, maximum values of the real part of dielectric constant $\varepsilon_1(\omega)$, the imaginary part of dielectric constant $\varepsilon_2(\omega)$, refractive index $n(\omega)$, and reflectivity $R(\omega)$ for TiS_2 for $E//x$ and $E//z$ within GGA.

	$\varepsilon_1(0)$	Maximum $\varepsilon_1(\omega)$	$n(0)$	Maximum $n(\omega)$	Energy range (eV) for $n(\omega)<1$	$R(0)$ (%)	Maximum $R(\omega)$ (%)
$E//x$	24.07	29.01	4.91	5.44	5.73–6.95 eV and $E>11.95$ eV	43	71
$E//z$	12.16	14.73	3.49	3.88	11.52–11.6 eV and $E>11.88$ eV	30	73

In conclusion, using an *ab initio* method called linearly increased plane waves (FP-LAPWs) in the framework of the theory of the density functional, we have studied the electronic properties of the TiS_2 material. We use the approximation GGA implanted in the WIEN2k code to determine the potential for exchange and correlation. The choice of this material is justified by the fact that it has often been studied in recent years to be used as the positive electrode in lithium batteries. Thus we investigate the electronic properties: the band structure and the DOS. Our electronic structure studies indicate that the TiS_2 material shows a metallic behavior. TiS_2 shows a significant optical conductivity in the energy range of 1.2–10 eV.

References

[1] Dolui K and Sanvito S 2013 *School Phys. AMBER CRANN Inst. Trinity College Dublin* **2** Ireland
[2] Qiao Y B, Zhong G H, Li D, Wang J L, Qin X Y and Zeng Z 2007 *Chin. Phys. Lett.* **24** 1050
[3] Let A L, Mainwaing D, Rix C and Murugaraj P 2007 *Rev. Roum. Chem.* **52** 235
[4] Beaumale M, Barbier T, Bréard Y, Guelou G, Powell A V, Vaqueiro P and Guilmeau E 2014 *Acta Mater.* **78** 86
[5] Güller F, Helman C and Llois A M 2012 *Physica* B **407** 3188
[6] Mainwaring D E, Let A L, Rix C and Murugaraj P 2006 *Solid State Commun.* **140** 355
[7] Amzallag E, Martinez H, Baraille I, Rérat M, Loudet M and Gonbeau D 2007 *Solid State Sci.* **9** 594
[8] Yu F, Sun J X and Zhou Y H 2010 *Solid State Sci.* **12** 1786
[9] Gatensby R, Mcevoy N, Lee K, Hallam T, Berner N C, Rezvani E, Winters S, O'Brien M and Duesberg G S 2014 *Appl. Surf. Sci.* **297** 139
[10] Let A L, Mainwaring D E, Rix C and Murugaraj P 2008 *J. Non-Cryst. Solids* **354** 1801
[11] Zhu Z, Cheng Y and Schwingenschlögl U 2013 *Phys. Rev. Lett.* **110** 077202
[12] Zhang Y, Li Z, Jia H, Luo X, Xu J, Zhang X and Yu D 2006 *J. Cryst. Growth* **293** 124
[13] Ryzhikov M R, Slepkov V A, Kozlova S G, Gabuda S P and Fedorov V E 2014 *Comput. Theor. Chem.* **1027** 125
[14] Li D, Qin X Y and Gu Y 2006 *Mater. Res. Bull.* **41** 282
[15] Ataca C, Sahin H and Ciraci S 2012 *J. Phys. Chem.* C **116** 8983
[16] Carmalt C J, Parkin I P and Peters E S 2003 *Polymer* **22** 1263
[17] Ivanovskaya V V and Seifert G 2004 *Solid State Commun.* **130** 175
[18] Li D, Qin X Y, Zhang J, Wang L and Li H J 2005 *Solid State Commun.* **135** 237
[19] Martinez H, Tison Y, Baraille I, Loudet M and Gonbeau D 2002 *J. Electron Spectrosc. Relat. Phenom.* **125** 181
[20] Fang C M, De Groot R A and Haas C 1997 *Phys. Rev.* B **56** 4455
[21] Murnaghan F D 1944 *Proc. Natl. Acad. Sci. USA* **30** 244
[22] Ben Nasr T, Ben Abdellah H and Bennaceur R 2010 *Physica* B **405** 3427
[23] Amin B, Khenata R, Bouhemadou A, Ahmed I and Maqbool M 2012 *Physica* B **407** 2588